



## A Novel Approach for the De-Noising of Medical Images

C. Kalyana Chakravarti, G. Sumalatha, K. Sriraman

Department of CSE, JNTUK  
A.P., India

**Abstract:** *In medical images, noise suppression is a particularly delicate and difficult task. A tradeoff between noise reduction and the preservation of actual image features has to be made in a way that enhances the diagnostically relevant image content. The main properties of a good image de-noising model are that it will remove noise while preserving edges and contours. This paper proposes a new de-noising technique called Contourlet transform. This method of contourlets has been used extensively for de-noising medical image. It provides a flexible multi resolution, local and directional image expansion. The contourlet transform is realized efficiently via double iterated filter bank structure where the Laplacian Pyramid (LP) filter in the first stage is used to capture the point discontinuities, and then followed by a directional filter bank (DFB) to link the point discontinuities.*

*In this paper, we evaluate Contourlets de-noising procedures using medical test images corrupted with additive Gaussian noise, salt & pepper noise, multiplicative noise and compare the performance with FBP, Wavelets, in terms of the peak-signal-to-noise ratio (PSNR) as a measure of the quality of de-noising. Experimental results show that the contourlet transform outperforms the other two techniques.*

**Keywords:** *Contourlets, De-noising, FBP, Laplacian Pyramid (LP), Tomography, Wavelets.*

### I. INTRODUCTION

Interest in digital image processing methods stems from two principal application areas: improvement of pictorial information for human interpretation and processing of image data for storage, transmission, and representation for autonomous machine perception. An image is often corrupted by noise in its acquisition and transmission. Image de-noising is used to remove the noise while retaining as much as possible the important signal features. All de-noising methods show an outstanding performance when the image models corresponds to the algorithm assumptions, but fails in general and create artifacts or remove image fine structures. In the filtered back projection technique we are interested in the recovery of an image  $f$  from its tomographic projections  $Y$ , also called sinograms, and defined as:  $Y = R f + W$

Where  $f[n_1, n_2] \in \mathbb{C}^{N_1 \times N_2}$  is the observed image,  $W$  is an additive noise, usually modeled as Poisson or Gaussian noise, and  $R$  is the discrete Radon transform. The discrete Radon transform is derived from its continuous version  $R_c$ , which is equivalent to the X-ray transform in two dimensions and is defined as

$$P_{\theta}(t) = \int_{-\infty}^{\infty} \int_{-\infty}^{\infty} f(x,y) \delta(x \cos \theta + y \sin \theta - t) dx dy$$

Where  $f(x, y) \in \mathbb{R}^2$ ,  $\delta$  is the Dirac delta function and  $\theta \in [0, 2\pi]$ . In the discrete Radon transform, a line integral along  $x \cos \theta + y \sin \theta = t$  can be approximated by a summation of the pixel values inside the strip  $t - \frac{1}{2} < n_1 \cos \theta + n_2 \sin \theta < t + \frac{1}{2}$ . The generation of sinogram data corrupted by additive Gaussian noise is shown in Figure.1.

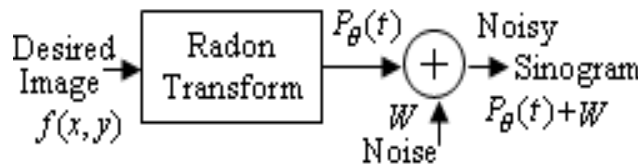


Fig.1 Generation of Noisy Sinogram

Computerized Tomography measure the density or the metabolic activity of a section of the patient's body (i.e., roughly speaking, produce sinograms  $Y$ ), and an estimation of the image  $f(x, y)$  representing the observed section is derived by a tomographic reconstruction procedure from the sinograms. This sinogram is filtered by using a ramp filter to eliminate the noise and then inverse radon transform is obtained which is also called as back projection to reconstruct the original image. The back projection technique suffers from blurring operator. FBP suffers from serious performance limitations, due to the fact that the vectors of the Fourier basis provide a good representation (diagonalization) of the Radon operator, but are not adapted to represent spatially inhomogeneous data such as medical images. A fundamental difficulty of tomographic reconstruction comes from the fact that the Radon transform is a smoothing transform, and inverting the Radon transform in presence of additive noise is an ill-posed inverse problem, because  $R^{-1}$  is not a bounded linear operator; numerically speaking, a direct computation of  $R^{-1}f$  would be contaminated by a huge additive noise  $z = R^{-1}W$ .

To improve the performance of tomographic reconstruction procedures, researchers have studied iterative statistical model based techniques. These approaches can provide a significant improvement over FBP. One of such technique is the Wavelet transform to estimate the signal from the noisy data. For, 1-D piecewise smooth signals like scan line of an image, 1-D wavelets have been established as the right tool. However natural images are not simple stacks of, 1-D piecewise smooth scan lines; discontinuity points that is edges are typically located along smooth curves that is contours owing to smooth boundaries of physical objects. As a result of separable extinction from 1-D bases wavelets in 2-D are good at isolated the discontinuities at edge points, but will not see smoothness along contours. The weakness of the wavelet domain is that it typically does not economically represent the noise. Therefore the wavelet shrinkage is unsatisfactory with large MSE; the estimate is either noisy or distorted. The limitations of commonly used separable extensions of 1-D transforms, such as Fourier and Wavelet transforms in capturing the geometry of image edges are well known.

In this paper we perceive a true 2-D transform called contourlet transform that can capture the intrinsic geometrical structure that is key in visual information. This method of contourlets has been used extensively for de-noising medical image. It provides a flexible multi resolution, local and directional image expansion. The contourlet transform is realized efficiently via double iterated filter bank structure where the Laplacian Pyramid (LP) filter in the first stage is used to capture the point discontinuities, and then followed by a directional filter bank (DFB) to link the point discontinuities.

## II. LIMITATIONS OF OTHER DENOISING TECHNIQUES

Filtered back projection (FBP) method of image de-noising uses inverse Radon transform. But the inversion of the radon transform in the presence of noise is numerically unstable in tomographic image reconstruction and is said to be ill conditioned. Wavelet transform, a multiscale transform is good at isolating the discontinuities at edge points, but will not see the smoothness along the contours.

The image de-noising techniques such as the steerable pyramid, brushlets which are multiscale and directional image representations do not allow for a different number of directions at each scale while achieving nearly critical sampling. The recently developed approaches for the efficient representations of geometrical regularity including the image de-noising techniques such as ridgelets, wedgelets, require an edge-detection stage, followed by an adaptive representation. By contrast, Curvelet representation is fixed transform. This feature allows it to be easily applied in a wide range of image processing tasks, similar to wavelets. The curve let construction simple in the continuous domain but causes the implementation for discrete images – sampled on a rectangular grid – to be very challenging. In particular, approaching critical sampling seems difficult in such discretized constructions.

## III. IMAGE DENOISING USING CONTOURLETS

The good image de-noising technique should posses the following 5 properties.

1. Multiresolution
2. Localization
3. Critical sampling
4. Directionality
5. Anisotropy.

Among these desired data the first three are successfully provided by separable wavelets, while the last two are provided by the contourlet transform. This contourlets uses nonseparable double filtered structure for obtaining the spares expansions for typical images having smooth contours. In this double filter bank the laplacian pyramid is first used to capture the points discontinuities ( multiresolution expansion ) and then followed by directional filter banks to link point discontinuities(multi directional expansion).

### 3.1 Review of Contourlet Transform

#### A. Pyramid frames

One way to obtain a multiscale decomposition is to used Laplacian pyramid (LP) .This LP decomposition at each level generates a down sampled low pass version of the original image and the prediction resulting in a band pass image. The following figure depicts this decomposition process where H and G are called (low pass) Analysis and synthesis filters, respectively and M is sampling matrix .the process can be iterated on the course (down sampled low pass) signal .in multidimensional filter banks ,sampling is represented by sampling matrices ; for example ,down sampling  $x[n]$  by M yields  $x_d[n] = x[Mn]$ , where M is an integer matrix.

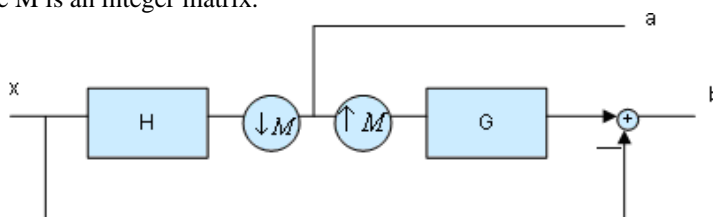


Fig:2 L-Pone level of decomposition

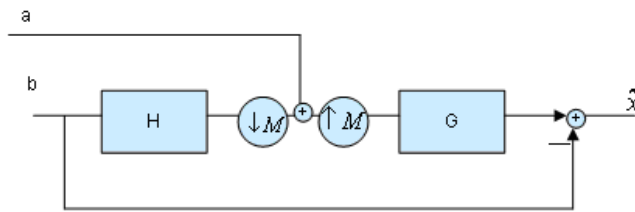


Fig:3 The new reconstruction scheme for the LP

The LP has distinguishing feature that this does not have scrambled frequencies. This frequency scrambling happens in the wavelets filter bank when a high pass channel, after down sampling is folded back into low frequency band and thus its spectrum is reflected. In the LP, this effect is avoided by down sampling the low pass channel only.

The LP orthogonal filters that is analysis and synthesis filters, or time reversal,  $h[n]=g[-n]$  and  $g[n]$  is orthogonal to it's translates with respect to sampling lattice by  $M$  provides a tight frame with frame bounds are equal to one. In this case, we proposed the use of optimal linear reconstruction using dual frame operator as shown in Fig.3. The new reconstruction differs from the usual method where the signal is obtained by simply adding back the difference to prediction from coarse signal and was shown to achieve significant improvement over usual reconstruction in presence of noise.

Iterated directional filter banks:

The directional filter banks (DFB) is efficiently implemented via an l-level binary tree decomposition that leads to  $2^l$  sub bands with wedge shaped frequency partitioning as shown in Fig.4

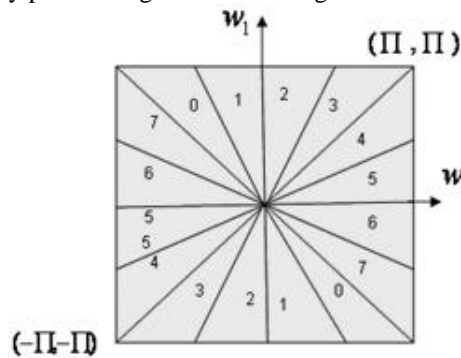


Fig:4

Directional filter bank frequency portioning where there are  $2^l=8$  real wedge-shaped frequency bands.

This DFB is constructed from two building blocks the first building block is a two channel quincunx filter banks with fan filters (see Figure.5) that divides a 2-D spectrum in to two directions: horizontal and vertical. The second building block is a shearing operator which amount to just reordering of image samples.

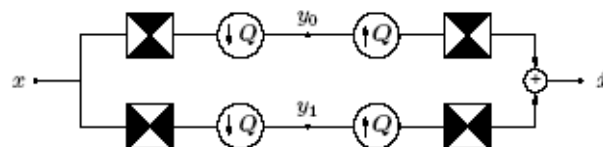


Figure.5 Two-dimensional spectrum partitioning using quincunx filter banks with fan filters. The black regions represent the ideal frequency supports of each filter.  $Q$  is a quincunx sampling matrix.

The following figure shows an application of shearing operator where a  $-45^\circ$  edge becomes a vertical edge.



Figure.6 Example of shearing operation that is used like a rotation operation for DFB decomposition. (a) The "cameraman" image. (b) The "cameraman" image after a shearing operation.

By adding a pair of shearing operators and its inverse (unshearing) to before and after, respectively, a two channel filter bank in Figure.5 we obtained a different directional frequency partition while maintaining perfect reconstruction. Thus the key in, the DFB is to use an approximate combination of shearing operators together with to direction partition of quincunx filter banks at each node in a binary tree structured filter bank, to obtain the desired 2-D spectrum division as

shown in the Figuer.4 Using multirate identities ,it is instructive to view an l-level tree structured DFB equivalently as a  $2^l$  parallel channel filter bank with equivalent filters and overall sampling matrices as shown in the Figure.7.Denote these equivalent (directional) synthesis filters as  $D_k^{(l)}, 0 \leq k < 2^l$  which correspond to the sub bands indexed as Figure.4.

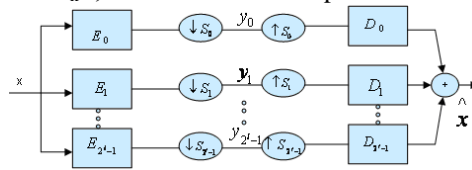


Figure.7 The multichannel view of an l-level tree-structured directional filter bank. The corresponding overall sampling matrices were shown to have following diagonal forms

$$S_k^{(l)} = \begin{cases} \text{diag}(2^{l-1}, 2) \text{ for } 0 \leq k < 2^{l-1} \\ \text{diag}(2, 2^{l-1}) \text{ for } 2^{l-1} \leq k < 2^l \end{cases}$$

Which means sampling is separable. The two sets correspond to the mostly horizontal and mostly vertical sets of directions, respectively. From the equivalent parallel view of the DFB, we see that the family

$$\{d_k^{(l)} [n - S_k^{(l)} m]\} 0 \leq k < 2^l, m \in Z^2$$

Obtained by translating the impulse responses of the equivalent synthesis filters  $D_k^{(l)}$  over the sampling lattices by  $S_k^{(l)}$  provides a basis for discrete signals in  $l^2(Z^2)$ . This basis exhibits both directional and localization properties.

We choose ‘9-7’biorthogonal filters because they have been shown to provide the best results fir images, partly because they are linear phase and are close to bring orthogonal. In the DFB stage we use the ‘23-45’ (‘pkva’) biorthogonal quincunx filters designed by Phoong, Kim, Vidyanathan, and Ansari and modulated them to obtain the biorthogonal fan filters. Apart from also being linear phase and nearly orthogonal, these fan filters are closed to having the ideal frequency response and thus can approximate the directional vanishing moment condition.

Multiscale and directional decomposition: The discrete contourlet transform.

Combining the Laplacian pyramid and the directional filter bank, we are now ready to describe their combination into a double filter bank structure .since the directional filter bank (DFB) was designed to capture the high frequency (representing directionality) of the input image , the low frequency content is poorly handled .in fact, with the frequency partition shown in Figure.4.,low frequency would leak into several directional sub bands ,hence the DFB alone does not provide a sparse representation for images. This fact provides another reason to combine the DFB with a multiscale decomposition, where low frequencies of input image are removed before applying the DFB. shows multiscale and directional decomposition using a combination of a Laplacian pyramid (LP) and a directional filter bank (DFB).band pass images from the LP are fed into a DFB so that directional information can be captured .The scheme can be iterated on the coarse image .The combined result is a doubled iterated filter bank structure, named contourlet filter bank, which decomposes images into directional sub bands at multiple scales.

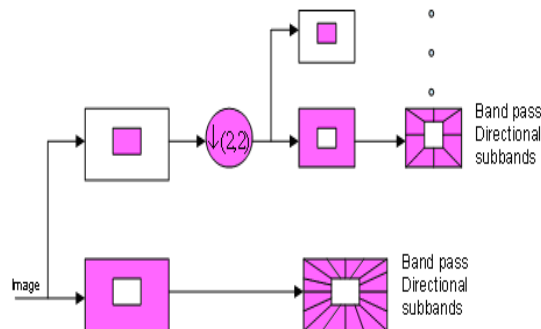


Figure.8. the contourlet filter bank: first, a multiscale decomposition into octave bands by the Laplacian pyramid is computed, and then a directional filter bank is applied to each band pass channel.

Specifically ,let  $a_0[n]$  be the input image .the output after the LP stage is J band pass images  $b_j[n]$ ,  $j = 1, 2, 3, \dots, J$  (in the fine –to–coarse order ) and a low pass image  $a_j[n]$ .that means , the j-th level of the LP decomposes the image  $a_{j-1}[n]$  into a coarser image  $a_j[n]$  and a detail image  $b_j[n]$  is further decomposed by an  $l_j$  level DFB into  $2^{l_j}$  ,Band pass directional image

$$C_{j,k}^{l_j} [n], k = 0, 1, 2, \dots, 2^{l_j} - 1.$$

Contourlets and directional multiresolution Analysis:

As for the wavelet filter bank , the contourlet filter bank has an associated continuous –domain expansion in  $L2(R^2)$  using the contourlet functions .The new elements in the frame work are multidirection and it’s combination with multi scale .For simplicity, we will only consider the case with orthogonal filters , which leads tight frames .

We start with the multiresolution analysis for the LP, which is similar to the one for wavelets. Suppose that the LP in the contourlet filter bank uses orthogonal filters by 2 in each dimension (that means  $M = \text{diag}(2, 2)$  in figure 2). Under certain regularity conditions, the low pass synthesis filter  $G$  in the iterated LP uniquely defines a unique scaling function  $\phi(t) \in L_2(\mathbb{R}^2)$  that satisfies the following two scale equation

$$\theta(t) = 2 \sum_{n \in \mathbb{Z}^2} g[n] \phi(2t - n)$$

Let

$$\phi_{j,n} = 2^{-j} \phi\left(\frac{t - 2^j n}{2^j}\right), j \in \mathbb{Z}, n \in \mathbb{Z}^2$$

Then the family is an orthonormal basis for an approximation subspace  $V_j$  at the scale  $2^j$ . Furthermore  $\{V_j\}_{j \in \mathbb{Z}}$  provide a sequence of multiresolution nested subspaces  $\dots V_2 \subset V_1 \subset V_0 \subset V_{-1} \subset V_{-2} \dots$ , where  $V_j$  is associated with uniform grid of intervals  $2^j \times 2^j$  that characterizes image approximation at scale  $2^j$ . The difference images in the LP contain the detail necessary to increase the resolution between two consecutive approximation subspaces. Therefore, the difference images live in a subspace  $W_j$  that is the orthogonal complement of  $V_j$  in  $V_{j-1}$ , or. In "Framing pyramids" we show that the LP can be considered as an over sampled filter bank where each polyphase component of difference image  $b[n]$  in figure 2, together with the coarse image  $a[n]$ , comes from a separate filter bank channel with the same sampling matrix  $\text{diag}(2, 2)$ . Let  $F_i(Z)$ ,  $0 \leq i \leq 3$  be synthesis filters for these polyphase components. These are high pass filters. As for wavelets, we associated with each of these filters a continuous functions  $\varphi^{(i)}(t)$  where

$$\varphi^{(i)}(t) = 2 \sum_{n \in \mathbb{Z}^2} f_i[n] \phi(2t - n)$$

Using the above equation we can say that if

$$\varphi_{j,n}^{(i)}(t) = 2^{-j} \varphi^{(i)}\left(\frac{t - 2^j n}{2^j}\right), j \in \mathbb{Z}, n \in \mathbb{Z}^2$$

Then for scale  $2^j$ ,  $\{\varphi_{j,n}^{(i)}\}_{0 \leq i \leq 3, n \in \mathbb{Z}^2}$  is a tight frame for  $W_j$ . For all scales,

$\{\varphi_{j,n}^{(i)}\}_{j \in \mathbb{Z}, 0 \leq i \leq 3, n \in \mathbb{Z}^2}$  is a tight frame for  $L_2(\mathbb{R}^2)$ .

In both cases the frame bounds are equals to 1.

### B. Multidirection

In the iterated contourlet filter bank, the discrete basis of the DFB can be regarded as a change of basis for the continuous domain subspaces for the multiscale analysis in the last section. Suppose that the DFB's in the contourlet bank uses orthogonal filters. Although in the contourlet transform the DFB is applied to difference images or the detail subspaces  $W_j$  we first show what happens when the DFB is applied to the approximation subspaces  $V_j$ . Suppose that

$\{P_{j,k,n}^{(l)}\}_{n \in \mathbb{Z}^2}$  is an orthonormal of subspace  $V_{j,k}^{(l)}$  to increase the directional resolution, an extra level of decomposition by pair of orthogonal filter is applied to the channel represented by that leads to two channels with equivalent filters  $d_k^{(l)}$  that leads to two channels with equivalent filters  $d_{2k}^{(l+1)}$  and  $d_{2k+1}^{(l+1)}$ . This transforms the orthonormal basis  $\{p_{j,k,n}^{(l)}\}_{n \in \mathbb{Z}^2}$ . Each of these families generates subspace with finer directional resolution.

So we can say that if

$P_{j,k,n}^{(l)}(t) = \sum_{m \in \mathbb{Z}^2} d_k^{(l)}[m - S_k^{(l)} n] \phi_{j,m}^{(l)}(t)$  for arbitrary but finite  $l$ . Then the family  $\{P_{j,k,n}^{(l)}\}_{n \in \mathbb{Z}^2}$  is an orthonormal basis of directional subspaces  $V_{j,k}^{(l)}$  for each  $K=0, 1, 2, \dots, 2^l - 1$ . Further more

$$V_{j,k}^{(l)} = V_{j,2k}^{(l+1)} \oplus V_{j,2k+1}^{(l+1)}$$

$$V_{j,k}^{(l)} \perp V_{j,k'}^{(l)} \text{ For } K \neq k' \text{ and}$$

$$V_j = \bigoplus_{k=0}^{2^l - 1} V_{j,k}^{(l)}$$

### 3.2 Image De-noising using contourlet transforms

The improvement in approximation by contourlets based on keeping the significant coefficients will directly lead to improvement in applications, including compression, de-noising, and feature extraction. As an example, for image de-noising, random noise will generate significant wavelet coefficients just like true edges, but is less likely to generate significant contourlet coefficients. Consequently, a simple threshold scheme applied on the contourlet transform is more effective in removing the noise than it is for the wavelet transform.

The algorithm is

1. Choose the appropriate filters for pyramidal and directional decomposition.
2. Choose the no of levels in the pyramid levels of pyramid.
3. Choose the appropriate values for threshold (Th) and for noise level (rho).
4. Generate noisy image.
5. Perform multiscale and multidirectional decomposition on the noisy image.
6. Calculate the contourlet threshold by using the given threshold.
7. Apply threshold for noisy coefficients.
8. Perform multistage and multidirectional reconstruction to reconstruct the de-noised image.
9. Calculate the PSNR value to compare it with wavelet PSNR.

The contourlet transform is shown to be more effective in recovering smooth contours, both visually as well as in PSNR than wavelets.

#### IV. IMPLEMENTATION AND RESULTS

##### Implementation

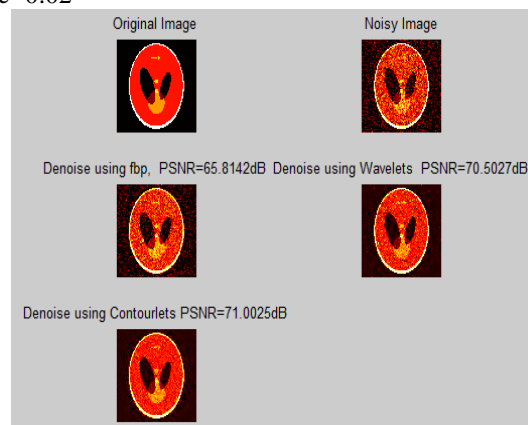
The well-known Shepp-Logan “head phantom” of size 256 X 256, “chest phantom” of size 256 X 256, “Kidney phantom” of size 256 X 256, is taken as test images. The number of angles is 256 and the number of projections is 256. The three types of noise, Gaussian of different means and different variances, salt & pepper of different densities are added to the test image. The algorithms of FBP, wavelets and contourlets are implemented in MATLAB. The performance of these algorithms is compared by using peak signal to noise ratio (PSNR) value. Contourlets are shown to be superior compared to wavelets in capturing fine contours. In addition to there is significant gain in PSNR for contourlets.

##### Results

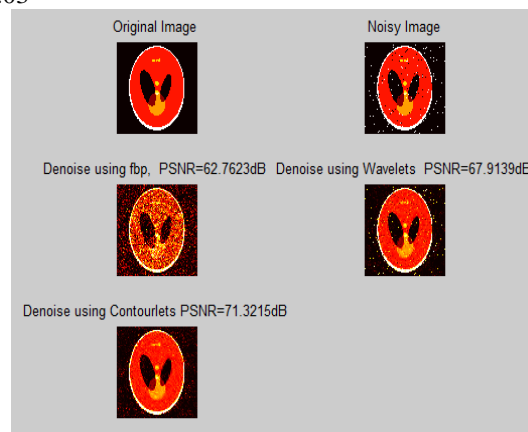
The results of all the 3 algorithms FBP, wavelets, contourlets when those are applied to de-noise the head phantom, chest phantom, Kidney phantom image having different properties of noises are given below.

##### Head Phantom

Gaussian noise of mean=0, variance=0.02

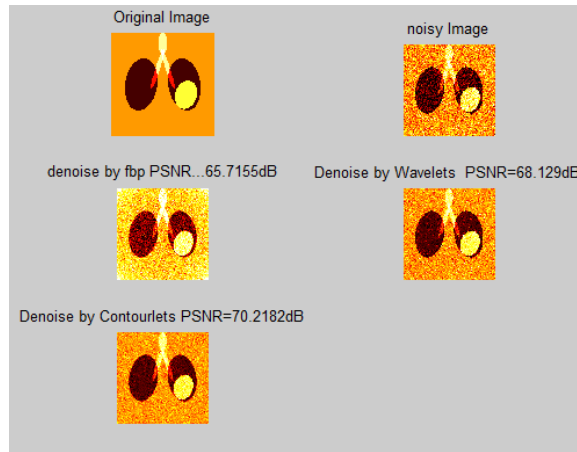


Salt & pepper noise of density of 0.03

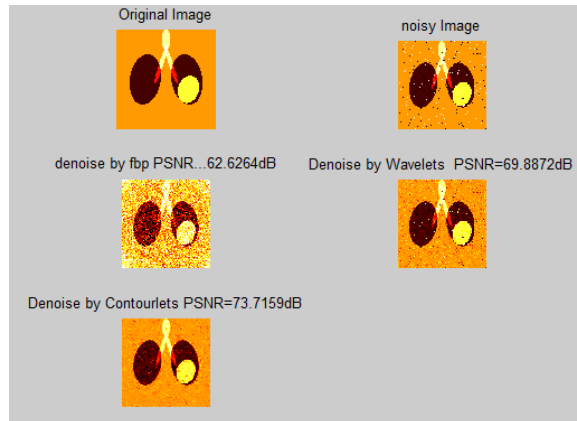


##### Chest Phantom

Gaussian noise of mean=0, Variance=0.02

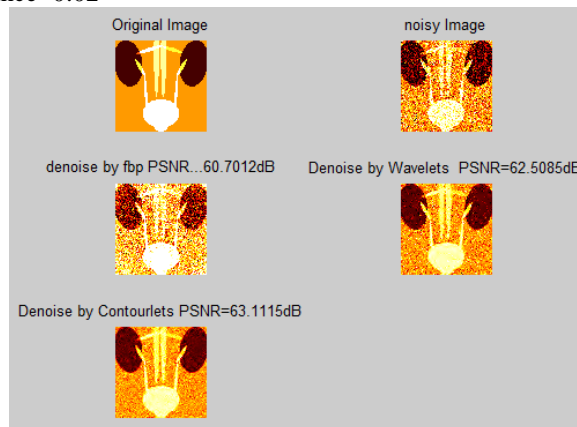


Salt & pepper noise of density of 0.03

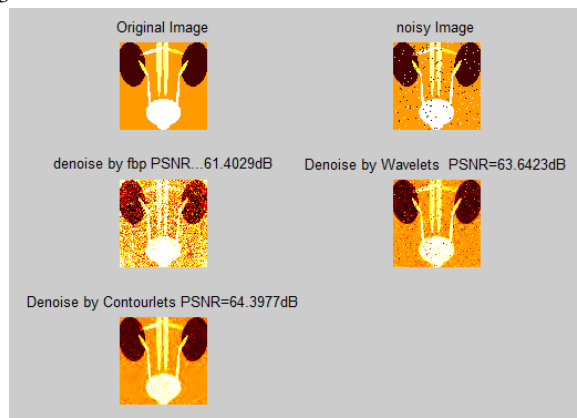


### Kidney Phantom

Gaussian noise of mean=0, Variance=0.02



Salt pepper noise of density =0.03



Performance tables

**De-noising of Head phantom**

Table-1

| Type of Noise                            | De-noise using FBP PSNR(db) | De-noise using Wavelets PSNR(db) | De-noise using Contourlets PSNR(db) |
|--|-----------------------------|----------------------------------|-------------------------------------|
| Gaussian noise of mean=0, variance=0.02. | 65.8142                     | 70.5027                          | 71.0025                             |
| Salt & pepper noise of density of 0.03   | 62.7623                     | 67.9139                          | 71.3215                             |

**De-noising of Chest phantom**

Table-2

| Type of Noise                            | De-noise using FBP PSNR(db) | De-noise using Wavelets PSNR(db) | De-noise using Contourlets PSNR(db) |
|--|-----------------------------|----------------------------------|-------------------------------------|
| Gaussian noise of mean=0, variance=0.02. | 65.7155                     | 68.1290                          | 70.2182                             |
| Salt & pepper noise of density of 0.03   | 62.6264                     | 69.8872                          | 73.7159                             |

**De-noising of kidney phantom**

Table-3

| Type of noise                            | De-noise using FBP PSNR(db) | De-noise using wavelets PSNR(db) | De-noise using contourlets PSNR(db) |
|--|-----------------------------|----------------------------------|-------------------------------------|
| Gaussian noise of mean=0, variance=0.02. | 60.7012                     | 62.5085                          | 63.1115                             |
| Salt & pepper noise of density of 0.03   | 61.4029                     | 63.6423                          | 64.3977                             |

**V. CONCLUSIONS**

The limitations of commonly used separable extensions of 1-D transforms, such as Fourier and Wavelet transforms in capturing the geometry of image edges are well known. This project dealt with a new 2-D image de-noising technique called contourlet transform which is very efficient in capturing the intrinsic geometrical structure like edges, that is key in visual information. The Implementation and Results of all algorithms are given. And the performances of these algorithms are compared by using peak signal to noise ratio (PSNR) value. Contourlets are shown to be superior compared to wavelets in capturing fine contours. In addition to there is significant gain in PSNR for contourlets.

**ACKNOWLEDGMENT**

The author wish to thank Dr. K. Phaneendra Kumar, principal of Vignan’s Lara Institute of Technology and Science, Mrs. G. Sandhya, Assoc.Prof. department of ECE of Vignan’s Lara Institute of Technology and Science Vadlamudi for their constant encouragement to this work.

**REFERENCES**

- [1] Minh N. Do and Martin Vetterli, “The contourlet transform: An efficient directional multiresolution image representation,”IEEE Trans. on Image Processing, to appear, 2004
- [2] Javier Portilla, Vasily Strela, Martin J. Wainwright, and Eero P. Simoncelli” Image Denoising Using Scale Mixtures of Gaussians in the Wavelet Domain” IEEE Trans.on Image Processing vol. 12, no. 11,November 2003
- [3] Jean-Luc Starck, Emmanuel J. Candès, and David L. Donoho ”The Curvelet Transform for Image Denoising” IEEE Trans.on Image Processing,vol.11,no.6,June 2002.
- [4] Elsa D. Angelini, Jérôme Kalifa, Andrew F. Laine “Harmonic Multiresolution Estimators For De-noising And Regularization Of Spect-pet data ”Presented at the IEEE International Symposium on Biomedical Imaging, Washington D.C., USA, 2002.

- [5] Boaz Matalon, Michael Zibulevsky, and Michael Elad, "Image de-noising with the Contourlet transform," in Proceedings of the SPIE conference wavelets, July 2005, vol. 5914.
- [6] Farrokh Rashid-Farrokhi, Student Member, IEEE, K. J. Ray Liu, Senior Member, IEEE, Carlos A. Berenstein, and David Walnut" Wavelet-Based Multiresolution Local Tomography" IEEE Trans.on Image Processing vol. 6, no. 10, October 1997
- [7] A.C.Kak and M.Slaney, "Principles Of Computerized Tomographic imaging", 3,49, IEEE press, (1987).
- [8] Lakhwinder Kaur Savita Gupta R.C. Chauhan' Image Denoising using Wavelet Thresholding"
- [9] L. Demaret, F. Friedrich, H. FÄuhr and T. Szygowski "Multiscale wedgelet denoising algorithms"
- [10] Rafael C.Gonzalez , Richard E.Woods, " Digital Image Processing",7,351- 352,Pearson education, (2003)
- [11] The math works, Inc, "Contourlet toolbox",<http://www.mathworks.com>.

#### **AUTHORS PROFILE**

- [1] **C. Kalyana Chakravarti**, M.Tech in vignan's Lara Institution of Technology & science. My research includes Image processing, Data mining and Networks.
- [2] **G. Sumalatha**, Asst. Professor, CSE in vignan's Lara Institution of Technology & science. His research includes Networks, Image Processing, and Digital Forensics.
- [3] **K. Sriraman**, MIEEE, MCS, MCIS, LMISTE (LM41052), MCSI currently working as a Assoc. Professor, Department of Computer Science and Engineering at Vignan's Lara Institute of Technology and Science, Vadlamudi, Guntur, A.P.,India. His Research Interests are Soft Computing, Artificial Intelligence, Image Processing, Neural Networks, Pattern Recognition, and Security.